

CAN WE DERIVE AN ABUNDANCE INDEX FOR THE SILKY SHARK BASED ON ITS ASSOCIATIVE BEHAVIOR WITH FLOATING OBJECTS?

Alexandra Diallo¹, Mariana Travassos Tolotti^{1,*}, Philippe Sabarros¹, Laurent Dagorn¹
Jean-Louis Deneubourg² and Manuela Capello¹

¹Institut de Recherche pour le Développement (IRD), UMR MARBEC (IRD, Ifremer, Univ. Montpellier, CNRS), Sète - France

²Unité d'Ecologie Sociale, Université Libre de Bruxelles, Campus de la Plaine, Bruxelles, Belgium

*Corresponding author, email: mariana.travassos@ird.fr

Abstract

Using data from the French tropical tuna purse seine fishery, this study proposes a new method to derive an abundance index for silky shark's populations. Two models were used: the first one describes the dynamics of sharks associated to floating objects (FOBs) used by tuna purse seiners in a social and in a non-social case. The second one illustrates the exchanges of individuals between the FOB-associated population and an external pool of sharks. The parameters estimates of the first model were obtained with fitting analysis. These parameters were then integrated into the second model. By approximating an unknown parameter (γ'), abundance indices were derived. This approach also allowed the construction of short-term temporal series relative to a reference year. This methodology has the potential to be applied to any other species associating with FOBs and serve as a tool for fisheries management.

Keywords

Abundance index; silky shark; floating objects; social behavior; tropical tuna purse seine fishery

1. Introduction

Ranked as vulnerable to near threatened on the IUCN red list, the silky shark (*Carcharhinus falciformis*) is a pelagic species distributed in tropical waters and vulnerable to tropical tuna fisheries. It is mainly caught as bycatch by pelagic longlines and gillnets, being also commonly captured by purse seiners (Fonteneau et al., 2013; Restrepo et al., 2017).

The European tropical purse seine fishery is currently one of the most modern and powerful fisheries in the world, accounting for 64% of the 4.7 million tons of tunas caught worldwide every year (Justel-Rubio et al., 2017). Two main types of tuna schools are targeted by the purse seiners: (i) free-swimming schools, generally monospecific, composed of larger individuals; and (ii) schools associated with floating objects (FOBs), that are multispecific and composed of smaller individuals (Dagorn et al., 2013b; Fonteneau et al., 2013). To date, 40 to 60% of the world's annual tropical tuna catches come from fishing sets on FOBs and between 50 and 100 thousands FOBs are deployed worldwide every year (Dagorn et al., 2013a; Filmlalter et al., 2013; Fonteneau et al., 2013).

There are between 2.8 to 6.7 times more bycatch on FOB-associated sets than on free-swimming schools sets (Dagorn et al., 2013b). Elasmobranchs account for about 5% of the total tuna biomass caught under FOBs, with the silky shark representing 90% of the catches of this group (Gilman, 2011). Recent estimates suggest that the total annual catch of silky sharks within the purse seine tropical tuna fisheries can reach up to 1,280 tons in the Indian Ocean and up to 39 tons in the Atlantic (Restrepo et al., 2017). Information regarding the state of the population of silky sharks is needed in order to assess the impact of the purse seine fisheries on this species.

The aim of this study is to develop a methodology to derive an abundance index for the silky shark using catch data from the tropical tuna purse seine fishery around FOBs collected by on board observers Atlantic and Indian oceans. Two main objectives are targeted: (i) determine the association dynamics of silky shark around FOBs through model comparisons; and (ii) derive an abundance index based on the exchanges of individuals between the FOB-associated population and an external pool of sharks using the parameters estimated by the best models describing the association dynamics.

2. Data preparation

Observer data from the French tropical tuna purse seine fleet, spanning from 2005 and 2017 in the Atlantic and Indian oceans, were used in the analyses (Figure 1). The data was made available by the Observatory of Exploited Pelagic Tropical Ecosystems (Ob7) of IRD (*Institut de Recherche pour le Développement*). Only sets on floating objects (FOBs) were considered in the analyses.

The total number of silky sharks caught under a single FOB set was used to classify catch events, starting from sets with zero silky shark occurrence up to sets with 20 silky sharks. The proportion of each catch event in relation to the total number of FOB sets was then calculated and represented in the form of histograms.

Proportions of catch events were calculated for small-scale statistical units of time and space in which the local population of the silky shark could be considered homogeneous. Based on the residency time of silky sharks around FOBs (Filmlalter et al., 2015, 2011), the temporal window of all statistical units were set as one month. The spatial scale was defined by Kernel density estimations. Each statistical unit included at least 20 fishing sets and gathered a minimum of 5 classes of catch events.

A total of 89 statistical units were defined, 30 in the Atlantic Ocean and 59 in the Indian Ocean. In the Atlantic Ocean the statistical units spanned from May 2012 to April 2017, while in the Indian Ocean they spanned from November 2006 and May 2017. An example of statistical unit with its respective catch events histogram is shown in Figure 2.

3. Modeling silky shark's dynamics around FOBs

Two models were used to describe the dynamics of silky sharks around FOBs. In the first model, silky sharks were considered to display social behavior, while in the second one they were considered to be non-social. The social behavior was modeled as a change in the residence time of a silky shark associated with a FOB when a certain number of congeners are present. This approach follows the postulate that the probability of a silky shark to leave a FOB will decrease if other silky sharks are also present at the same FOB. For the non-social scenario we hypothesized that the presence of congeners will not influence the residence time.

3.1. Social model

Considering X a discrete random variable representing “the associated population of sharks at a FOB” and Ω a threshold of sociability, the dynamics of X was modeled according to the conceptual scheme shown in Figure 3. At each time step, a FOB with a population of $X=i$ can gain a shark with a constant probability α , and can lose a shark with a probability $i \lambda_1$, if $i \leq \Omega$, and a probability $i \lambda_2$, if $i > \Omega$, with $\lambda_1 > \lambda_2$. Considering that the system is at equilibrium, the probability $P(X=i)$ for a FOB to be at a state i is:

$$\left\{ \begin{array}{l} P(0) = \frac{1}{\sum_{i=0}^{\Omega} \frac{1}{i!} \left(\frac{1}{l_1^i} - \frac{l_2^{\Omega}}{l_1^{\Omega}} \frac{1}{l_2^i} \right) + \frac{l_2^{\Omega}}{l_1^{\Omega}} e^{-(1/l_2)}} \\ P_{i \leq \Omega}(X = i) = \frac{1}{i! l_1^i} P(0) \\ P_{i > \Omega}(X = i) = \frac{1}{i!} \frac{1}{l_1^{\Omega} l_2^{i-\Omega}} P(0) \end{array} \right. \quad (\text{Equation 1})$$

With $\frac{\lambda_1}{\alpha} = l_1$ and $\frac{\lambda_2}{\alpha} = l_2$

3.2. Non-social model

The non-social model corresponds to the social model shown in Equation 1 with $l_1 = l_2 = l$ (or $\Omega = 0$). Similarly to the social model, the probability for a FOB to gain a shark is constant and is represented by α . In this case the probability $P(X=i)$ becomes:

$$\left\{ \begin{array}{l} P(0) = e^{-(1/l)} \\ P(X = i) = \frac{1}{i!} \left(\frac{1}{l} \right)^i P(0) \end{array} \right. \quad (\text{Equation 2})$$

By substituting $P(0)$ into the second equation we find $P(X = i) = \frac{1}{i!} \left(\frac{1}{l} \right)^i e^{-(1/l)}$, which is equivalent to a Poisson probability density function $X \sim P\left(\frac{1}{l}\right)$.

3.3. Fitting the probability functions

The distributions of catch events defined for each statistical unit were fitted with the probability functions shown in the equations above (Equations 1 and 2). Fits were used to determine which model (social and non-social) best described the observed

distributions. For the social model, fits were also used to define the best Ω value. A total of 5 social models were tested with $\Omega \in [1,5]$. The fits were conducted using Maximum Likelihood for non-linear models, through the nlsLM function of the minpack.lm package in R. Models with non-significant parameters were excluded from the comparisons. For the remaining models, best fits were chosen based on AIC values and qq-plots.

Most catch event distributions were best fitted by the social model with a social threshold (Ω) equal to 1, reaching 73% in the Atlantic and 64% in the Indian Ocean (Table 1). Together, the best-fitted social models ($\Omega \in [1,3]$) described 98% of all distributions. The models with a social threshold of 4 and 5 were never classified as best fits because one of their parameters (l_2) was always non-significant. The Poisson function (non-social model) only provided the best fit for one distribution in the Indian Ocean. An example of a comparative analysis between two fits is shown in Figure 4.

Table 1. Proportion of statistical units best fitted by each model (P= Poisson – non-social; S= social).

Ocean	Atlantic			Indian			
Function	P	S $\Omega=1$	S $\Omega=2$	P	S $\Omega=1$	S $\Omega=2$	S $\Omega=3$
Best fit (%)	0	73	27	2	64	29	5

4. Deriving an abundance index for the silky shark

Considering a set of N_{FOB} and a population of N_s silky sharks, the dynamics of the number of sharks X_j at FOB j (Figure 5) can be expressed as the following differential equation:

$$\frac{dX_j}{dt} = \mu_j X_e - \theta_j X_j \quad (\text{Equation 3})$$

where X_e is the unassociated population, μ the individual probability for a shark to join a FOB and θ the individual probability for a shark to leave a FOB. The social interactions are accounted at the level of the individual probability to leave a FOB (similar to the model shown in Eq. 1), considering that the probability θ_j is equal to θ_1 or θ_2 depending if the associated population is lower or higher than Ω . The total associated population can be written as $X_a = \sum_{j=1}^{N_{FOB}} X_j$ with N_{FOB} being the number of FOBs in the system and $N_s = X_e + X_a$ the total population of sharks. Notice that it is possible to relate the models in Equation 1 and Equation 3 considering $\theta_1 = \lambda_1$ and $\alpha = \mu X_e$.

The evolution in time of the associated population X_a can be written as:

$$\frac{dX_a}{dt} = N_{FOB} \mu X_e - \theta_1 X_\Omega - \theta_2 X_S \quad (\text{Equation 4})$$

with X_Ω being the total number of sharks associated to FOBs j having $X_j \leq \Omega$, i.e. the total number of sharks associated with FOBs below the sociality threshold. Similarly, $X_S = X_a - X_\Omega$ corresponds to the total number of sharks associated to FOBs j having $X_j > \Omega$. At equilibrium, Equation 4 can be written as:

$$X_e = \frac{\theta_1}{N_{FOB} \mu} X_\Omega + \frac{\theta_2}{N_{FOB} \mu} X_S \quad (\text{Equation 5})$$

Substituting Equation 5 into $N_s = X_e + X_a$ and considering that $X_a = X_\Omega + X_S$, the total population of sharks can be expressed as:

$$N_s = \left[1 + \frac{\theta_1}{N_{FOB} \mu}\right] X_\Omega + \left[1 + \frac{\theta_2}{N_{FOB} \mu}\right] X_S \quad (\text{Equation 6})$$

Note that, in the above equation, the total number of FOBs is a key variable to assess shark abundance. Quantifying FOB numbers remains a challenge and, although efforts have been made (Dagorn et al., 2013a; Fonteneau et al., 2013; Maufroy et al., 2015), available estimates are uncertain. To simplify this problem, the total number of FOBs could be expressed by an index of FOB density as $N_{FOB} = f i_{NFOB}$, with i_{NFOB} being the FOB-density index and f being a coefficient relating the FOB-density index with the total number of FOBs.

The total shark population associated below/above the sociality threshold can be expressed as:

$$\begin{cases} X_\Omega = N_{FOB} \sum_{i \leq \Omega} i P(X = i) = N_{FOB} \Psi(X_\Omega) \\ X_S = N_{FOB} \sum_{i > \Omega} i P(X = i) = N_{FOB} \Psi(X_S) \end{cases} \quad (\text{Equation 7})$$

where $\Psi(X_\Omega) = \sum_{i \leq \Omega} i P(X = i)$ and $\Psi(X_S) = \sum_{i > \Omega} i P(X = i)$, with $P(X = i)$ being the probability to find a FOB occupied by $X = i$ sharks, see Equation 1. Substituting the FOB-density index and Equation 7 into Equation 6, we arrive at the following abundance index:

$$N_s = f \left[\Psi(X_\Omega) (i_{NFOB} + \gamma') + \Psi(X_S) \left(i_{NFOB} + \frac{\gamma'}{c} \right) \right] \quad (\text{Equation 8})$$

with $\gamma' = \frac{\theta_1}{\mu f}$ and $c = \frac{\theta_1}{\theta_2} = \frac{l_1}{l_2}$

The values of $\Psi(X_\Omega)$, $\Psi(X_S)$ and c can be obtained from the histograms of the number of sharks per FOB and the fits, and the FOB-density index i_{NFOB} can be estimated.

Therefore, for each statistical unit corresponding to a given time t and area A , the above equation can be rewritten as:

$$\hat{N}_{s|t,A} = f \left[\hat{\Psi}_{t,A}(X_\Omega) (\hat{i}_{NFOB|t,A} + \gamma') + \hat{\Psi}_{t,A}(X_S) \left(\hat{i}_{NFOB|t,A} + \frac{\gamma'}{\hat{c}_{t,A}} \right) \right] \quad (\text{Equation 9})$$

This equation has still two unknowns: the coefficient f relating the FOB-density index with the total number of FOBs and γ' , that also depends on the probabilities of a shark to leave and reach a FOB (θ_1 and μ , respectively).

Considering that f and γ' do not vary in time, it is possible to obtain trends in the relative abundance of silky sharks for the same area (relative to a reference time) according to different values of γ' .

5. Deriving an abundance trend for the silky shark

We applied Equation 9 to three similar statistical units in the Indian Ocean, for which we disposed of enough samples over different years (Figure 6). For each year, a simple FOB-density index was derived, base on records of FOB encounters from observers' data. Such index corresponded to the total number of random FOB encounters recorded by the observers within the statistical unit, standardized by the sampling effort (total number of days at sea). A random encounter was defined as the encounter of a FOB of unknown ownership (i.e., a FOB of a fishing vessel/fleet different from the one of the observer).

Assuming a constant value of f , the abundance index, obtained for the years 2016 and 2017 relative to year 2007, was calculated as follows:

$$T = \frac{N_{s|t,A}}{N_{s|2007,A}} = \frac{\left[\hat{\Psi}_{t,A}(X_\Omega) (\hat{i}_{NFOB|t,A} + \gamma') + \hat{\Psi}_{t,A}(X_S) \left(\hat{i}_{NFOB|t,A} + \frac{\gamma'}{\hat{c}_{t,A}} \right) \right]}{\left[\hat{\Psi}_{2007,A}(X_\Omega) (\hat{i}_{NFOB|2007,A} + \gamma') + \hat{\Psi}_{2007,A}(X_S) \left(\hat{i}_{NFOB|2007,A} + \frac{\gamma'}{\hat{c}_{2007,A}} \right) \right]}$$

with $t \in [2015, 2017]$

(Equation 10)

The constant γ' in Equation 10 was considered as a parameter and a large range of values were tested [10^{-5} : 10^{15}]. The results in Figure 7 show two main trends, one for small values of γ' and other for large values. An intermediate zone can be identified between $\log(\gamma')=0$ and $\log(\gamma')=3$, where the index shows a larger variability.

Independently of the value of γ' , the temporal trends of the relative abundance index increased with time (Figure 7). For small γ' values (<1) the index varied from 1.8 in 2016/2007 to 2.4 in 2017/2007, whereas for large γ' values (>1000) the index increased from 1.4 to 3.2.

6. Remarks

By modeling silky shark's dynamics around FOBs we observed that 98% of the statistical units were best explained by a social behavior. In summary, silky sharks would stay associated with a FOB for a shorter period of time unless their corresponding social "threshold" was reached. The majority of cases (67%) were best explained by a social threshold of 1. This means that as soon as two sharks share a FOB, their residency time would increase. Studies using photography and video analysis, as well as acoustic telemetry, have described intraspecific interactions and movements of a range of species (Capello et al., 2011; Filmlalter et al., 2015; Mourier et al., 2012; Robert et al., 2013). These approaches could broaden the knowledge on silky sharks' social behavior around FOBs and help validate the social model.

For the first time, we could obtain a trend of relative abundance for silky sharks from data collected within the purse-seine fisheries that takes into account the associative behavior of the species. The obtained trends follow the same increasing pattern, although the magnitude of the increase varies depending on the value of γ' that is considered. Taking into account that $f \sim N_{FOB} \gg 1$ and that $\gamma' = \frac{\theta_1}{\mu_f}$, the regime of large γ' could only occur for $\theta_1 \gg \mu$, i.e. if the probabilities of departure from the FOB are much higher than the probability to reach a FOB. Such information, which is not available at the moment, could be obtained from electronic experiments measuring residence and absence times of silky sharks in an array of FOBs. For the moment, the electronic tagging data recorded for silky sharks can only provide estimates of residence times (Filmlalter et al., 2015).

Also, with those type of electronic tagging experiments, it would be possible to test whether the assumption of constant γ' (and thus constant probabilities to reach/depart from the FOB) holds. Indeed, external factors may also play an important role in the residency/absence times of silky sharks around FOBs. Juvenile

silky sharks are believed to use FOBs as shelter to hide from predators or as feeding point (Bonfil, 2008; Filmalter et al., 2017). Therefore, the presence of prey, as well as inter-specific associations could influence the probabilities to reach/depart from FOBs. Environmental factors could also play a role, as their influence on the species' catch rates have been shown (Lennert-Cody et al., 2018; Lopez et al., 2017).

7. Conclusion

In summary, the social model appears to better explain the presence of silky sharks at FOBs. Further field experiments could give a finer understanding of the mechanisms underlying silky shark's associative behavior, and also allow for a finer estimation of the model parameters. The model was nonetheless efficient in describing silky sharks' dynamics in a FOB environment, as well as in the derivation of a relative abundance index. Such analysis could be applied to larger datasets in order to derive longer time series. This modeling approach could be extended to other bycatch species to generate population trends and could be useful for future stock assessment analyses.

8. Acknowledgments

Data collection was ensured by the *Observatoire des Ecosystèmes Pélagiques Tropicaux Exploités* (Ob7) of IRD thanks to EU Data Collection Framework funding.

9. References

- Bonfil, R., 2008. The Biology and Ecology of the Silky Shark, *Carcharhinus Falciformis*, in: Camhi, M.D., Pikitch, E.K., Babcock, E.A. (Eds.), *Sharks of the Open Ocean*. Blackwell Publishing Ltd., Oxford, UK, pp. 114–127.
- Capello, M., Soria, M., Cotel, P., Deneubourg, J.L., Dagorn, L., 2011. Quantifying the interplay between environmental and social effects on aggregated-fish dynamics. *PLoS One* 6. doi:10.1371/journal.pone.0028109
- Dagorn, L., Bez, N., Fauvel, T., Walker, E., 2013a. How much do fish aggregating devices (FADs) modify the floating object environment in the ocean? *Fish. Oceanogr.* 22, 147–153. doi:10.1111/fog.12014
- Dagorn, L., Holland, K.N., Restrepo, V., Moreno, G., 2013b. Is it good or bad to fish with FADs? What are the real impacts of the use of drifting FADs on pelagic marine ecosystems? *Fish Fish.* 14, 391–415. doi:10.1111/j.1467-2979.2012.00478.x
- Filmalter, J., Cowley, P., Forget, F., Dagorn, L., 2015. Fine-scale 3-dimensional movement behaviour of silky sharks *Carcharhinus falciformis* associated with

- fish aggregating devices (FADs). Mar. Ecol. Prog. Ser. 539, 207–223.
doi:10.3354/meps11514
- Filmalter, J.D., Capello, M., Deneubourg, J.L., Cowley, P.D., Dagorn, L., 2013. Looking behind the curtain: Quantifying massive shark mortality in fish aggregating devices. Front. Ecol. Environ. 11, 291–296. doi:10.1890/130045
- Filmalter, J.D., Cowley, P.D., Potier, M., Ménard, F., Smale, M.J., Cherel, Y., Dagorn, L., 2017. Feeding ecology of silky sharks *Carcharhinus falciformis* associated with floating objects in the western Indian Ocean. J. Fish Biol. 90, 1321–1337. doi:10.1111/jfb.13241
- Filmalter, J.D., Dagorn, L., Cowley, P.D., Taquet, M., 2011. First Descriptions of the Behavior of Silky Sharks, *Carcharhinus Falciformis*, Around Drifting Fish Aggregating Devices in the Indian Ocean. Bull. Mar. Sci. 87, 325–337. doi:10.5343/bms.2010.1057
- Fonteneau, A., Chassot, E., Bodin, N., 2013. Global spatio-temporal patterns in tropical tuna purse seine fisheries on drifting fish aggregating devices (DFADs): Taking a historical perspective to inform current challenges. Aquat. Living Resour. 26, 37–48. doi:10.1051/alr/2013046
- Gilman, E.L., 2011. Bycatch governance and best practice mitigation technology in global tuna fisheries. Mar. Policy 35, 590–609. doi:10.1016/j.marpol.2011.01.021
- Justel-Rubio, A., Recio, L., Restrepo, V., 2017. A snapshot of the large scale tropical tuna purse seine fishing fleets as of June 2017. Washington, D.C.
- Lennert-Cody, C.E., Clarke, S.C., Aires-da-Silva, A., Maunder, M.N., Franks, P.J.S., Román, M., Miller, A.J., Minami, M., 2018. The importance of environment and life stage on interpretation of silky shark relative abundance indices for the equatorial Pacific Ocean. Fish. Oceanogr. 1–11. doi:10.1111/fog.12385
- Lopez, J., Alvarez-Berastegui, D., Soto, M., Murua, H., 2017. Modelling the Oceanic Habitats of Silky Shark (*Carcharhinus Falciformis*), Implications for Conservation and Management. Indian Ocean Tuna Comm.
- Maufroy, A., Chassot, E., Joo, R., Kaplan, D.M., 2015. Large-Scale Examination of Spatio-Temporal Patterns of Drifting Fish Aggregating Devices (dFADs) from Tropical Tuna Fisheries of the Indian and Atlantic Oceans. PLoS One 10, e0128023. doi:10.1371/journal.pone.0128023
- Mourier, J., Vercelloni, J., Planes, S., 2012. Evidence of social communities in a spatially structured network of a free-ranging shark species. Anim. Behav. 83, 389–401. doi:10.1016/j.anbehav.2011.11.008
- Murua, H., Abascal, F.J., Amande, J., Ariz, P., Bach, P., Chavance, P., Coelho, R., Korta, M., Poisson, F., Santos, M.N., 2013. Provision of scientific advice for the purpose of the implementation of the EUPOA sharks. Final Report. European Commission, Studies for Carrying out the Common Fisheries Policy (MARE/2010/11-LOT 2).
- Restrepo, V., Dagorn, L., Itano, D., Justel-Rubio, A., Moreno, G., Forget, F., 2017. A summary of bycatch issues and ISSF mitigation initiatives to-date in purse seine fisheries, with emphasis on FADs. Washington, D.C.
- Robert, M., Dagorn, L., Filmalter, J.D., Deneubourg, J.L., Itano, D., Holland, K., 2013. Intra-individual behavioral variability displayed by tuna at fish aggregating devices (FADs). Mar. Ecol. Prog. Ser. 484, 239–247. doi:10.3354/meps10303

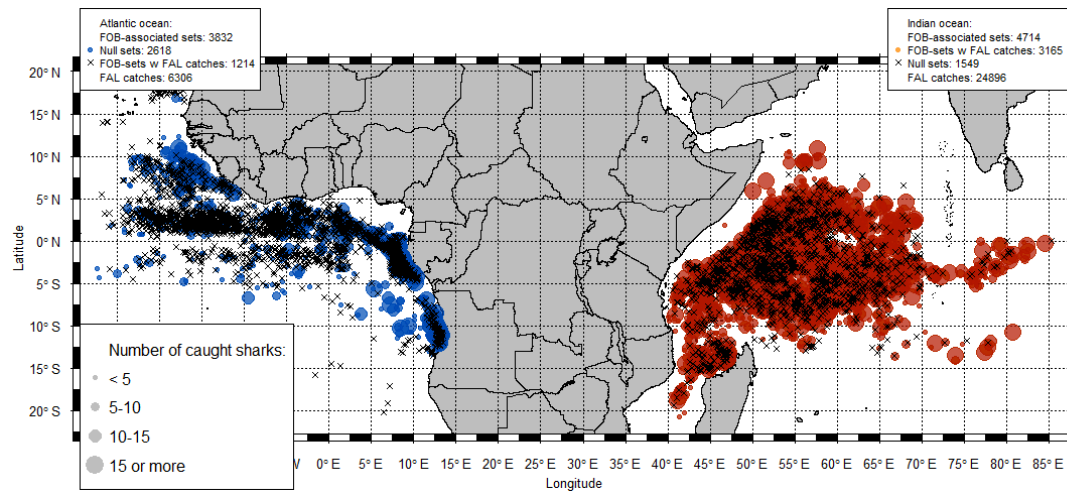


Figure 1. Silky shark captures by set between 2005 and 2017. Crosses represent sets without any capture of silky sharks and circles are proportional to the number of sharks caught within a set.

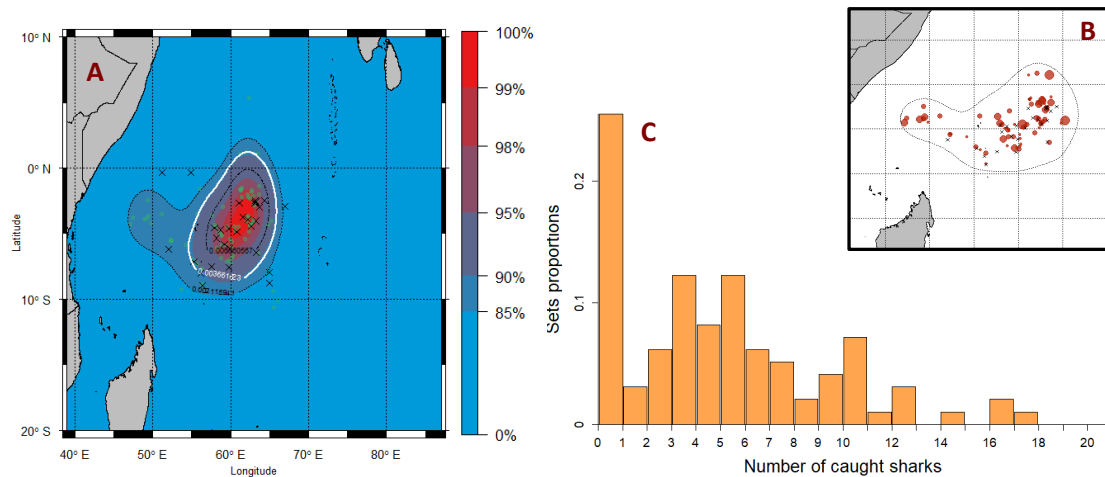


Figure 2. Example of statistical unit. Panel A shows the kernel density estimation obtained for the Indian Ocean in January 2016, with white contours defining the 95% quartile of cumulated density; Panel B shows the retained statistical unit; and panel C shows the corresponding catch events histogram.

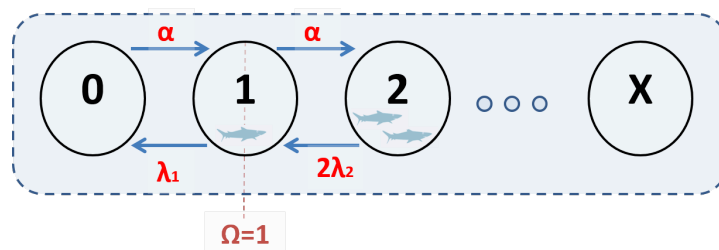


Figure 3. Conceptual model describing the change of state of a FOB in a social scenario. The numbers within each circle represent the number of associated sharks (X). In this example the sociability threshold is equal to 1.

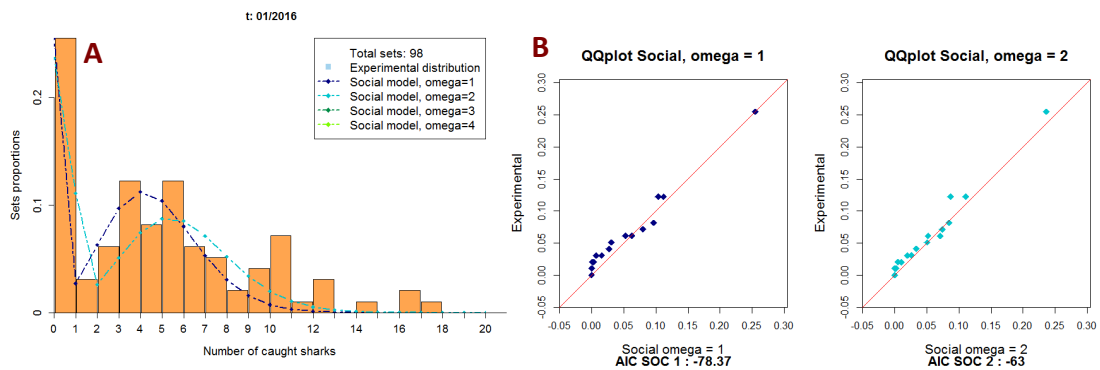


Figure 4. Example of a comparative analysis between two social models fitted to a statistical unit of the Indian Ocean (January 2016). Panel A illustrates the observed distribution of catch events extracted from the statistical unit. Panel B shows qq-plots and AICs of fitted models. The comparisons were limited to models where all parameters were significant. In this example, the model with a social threshold of 1 provides the best fit.

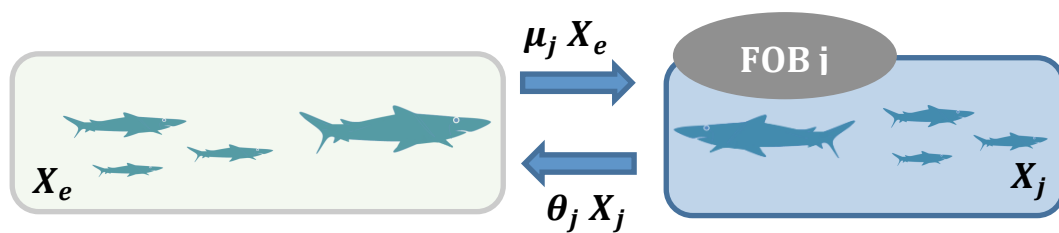


Figure 5. Conceptual model describing the dynamics of a silky sharks' population in a social scenario.

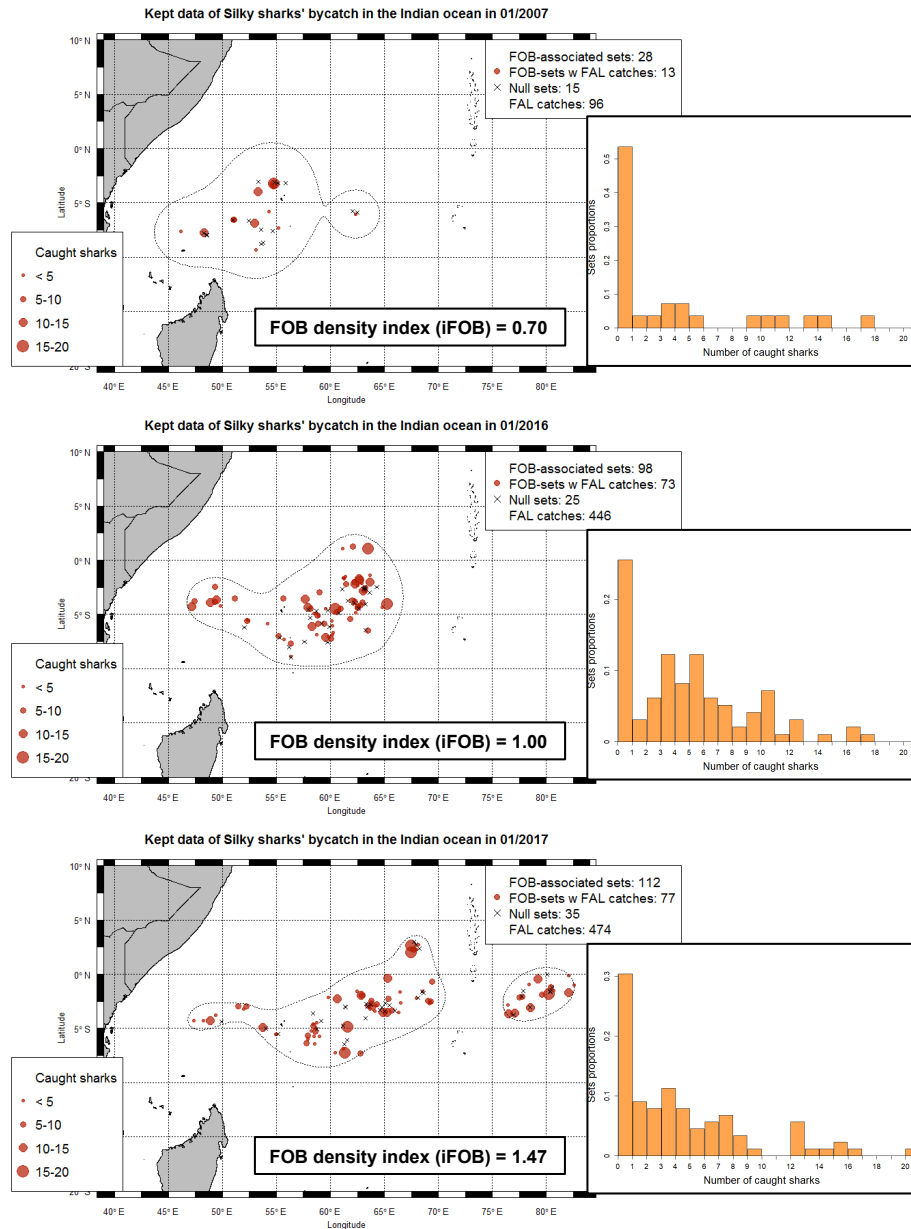


Figure 6. Statistical units used on the derivation of the abundance trends. The histograms represent the distribution of catch events within each statistical unit,

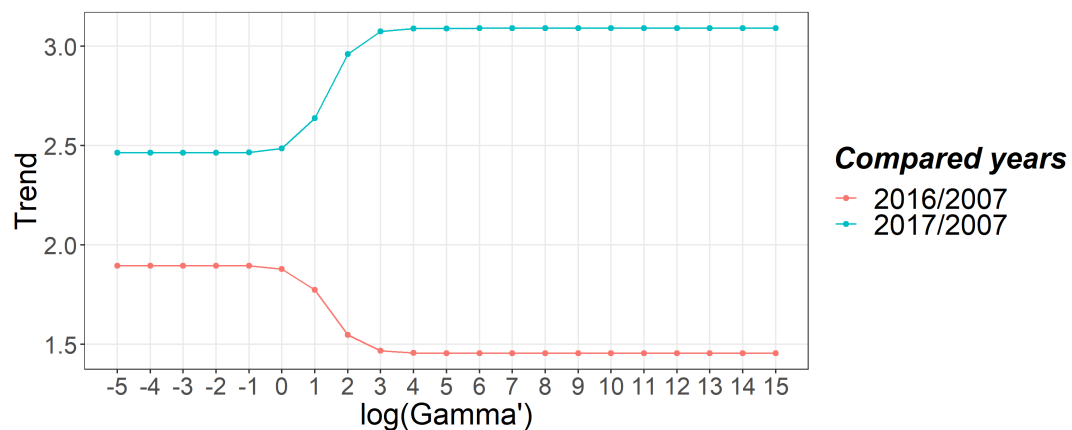


Figure 7. Changes in the trends of silky shark abundance following a range of values of γ' .

Supplementary material

$$\frac{dP(0)}{dt} = -\Psi(0,1)P(0) + \Psi(1,0)P(1)$$

$$\frac{dP(1)}{dt} = \Psi(0,1)P(0) - \Psi(1,0)P(1) - \Psi(1,2)P(1) + \Psi(2,1)P(2)$$

.....

$$\frac{dP(i)}{dt} = \Psi(i-1,i)P(i-1) - \Psi(i,i-1)P(i) - \Psi(i,i+1)P(i) + \Psi(i+1,i)P(i+1)$$

Where $\Psi(i-1, i)$ is the probability that a FOB, with already $i-1$ associated sharks, gains a shark and $\Psi(i, i-1)$ is the probability of a FOB with i associated sharks loses a shark.

Stationary distribution:

$$P(1) = \frac{\Psi(0,1)}{\Psi(1,0)} P(0)$$

$$P(2) = \frac{\Psi(1,2)}{\Psi(2,1)} P(1)$$

.....

$$P(i) = \frac{\Psi(i-1,i)}{\Psi(i,i-1)} P(i-1)$$

$$P(1) = \frac{\Psi(0,1)}{\Psi(1,0)} P(0)$$

$$P(2) = \frac{\Psi(1,2)}{\Psi(2,1)} \frac{\Psi(0,1)}{\Psi(1,0)} P(0)$$

$$P(3) = \frac{\Psi(2,3)}{\Psi(3,2)} \frac{\Psi(1,2)}{\Psi(2,1)} \frac{\Psi(0,1)}{\Psi(1,0)} P(0) \dots$$

$$P(i) = \prod_{j=1}^i \frac{\Psi(j-1,j)}{\Psi(j,j-1)} P(0); i = 1, \dots$$

$$1 = \sum_{i=0}^{\infty} P(i) = P(0) \left(1 + \sum_{i=1}^{\infty} \prod_{j=1}^i \frac{\Psi(j-1,j)}{\Psi(j,j-1)} \right)$$

$$P(0) = \frac{1}{1 + \sum_{i=1}^{\infty} \prod_{j=1}^i \frac{\Psi(j-1,j)}{\Psi(j,j-1)}}$$

Assuming that the probability of loosing a shark $\Psi(j, j-1)$ is proportionnal to j :

$$\Psi(j, j-1)j\Lambda(j, j-1)$$

and that the probability of gaining a shark is constant α :

$$P(i) = \frac{\alpha^i}{i!} \prod_{j=1}^i \frac{1}{\Lambda(j, j-1)} P(0); i = 1, \dots$$

$$P(0) = \frac{1}{1 + \sum_{i=1}^{\infty} \frac{\alpha^i}{i!} \prod_{j=1}^i \frac{1}{\Lambda(j, j-1)}}$$

In case of Λ constant, it corresponds to a Poisson distribution.